DOI:
10.1007/s11243-016-0097-5

Document Version
Peer reviewed version

Hydrogenase biomimetics: Structural and spectroscopic studies on diphosphine-substituted derivatives of $Fe_2(CO)_6(\mu$-edt) (edt = ethanedithiolate) and $Fe_2(CO)_6(\mu$-tdt) (tdt = 1,3-toluenedithiolate)

Shahed Rana[1] · Shishir Ghosh[1,*] · Md. Kamal Hossain[1] · Ahibur Rahaman[1] · Graeme Hogarth[2,*] · Shariff E. Kabir [1,*]

[1] Department of Chemistry, Jahangirnagar University, Savar, Dhaka-1342, Bangladesh
[2] Department of Chemistry, King's College London, Britannia House, 7 Trinity Street, London SE1 1DB, UK

E-mail: skabir_ju@yahoo.com (SEK); sghosh_006@yahoo.com (SG); graeme.hogarth@kcl.ac.uk (GH)

Abstract

Reactions of a series of diphosphines with $Fe_2(CO)_6(\mu$-edt) (**1**) and $Fe_2(CO)_6(\mu$-tdt) (**2**) have been explored, the nature of the products being highly dependent upon the diphosphine. Reaction of **1** with bis(diphenylphosphino)methane (dppm) in acetonitrile at 82 ^oC affords monosubstituted $Fe_2(CO)_5(\kappa^1$-dppm)(μ-edt) (**3**) in which the phosphine occupies an apical site and disubstituted $Fe_2(CO)_4(\mu$-dppm)(μ-edt) (**4**) in which the phosphine is acting as a bridging ligand, while a similar reaction of **2** with dppm yields only $Fe_2(CO)_4(\mu$-dppm)(μ-tdt) (**5**). In contrast, **1** and **2** react with 1,2-bis(diphenylphosphino)ethane (dppe) to form the chelate complex $Fe_2(CO)_4(\kappa^2$-dppe)(μ-edt) (**7**) and $Fe_2(CO)_4(\kappa^2$-dppe)(μ-tdt) (**8**), respectively, in both the diphosphine binds in an apical-basal fashion to a single iron atom. A second product of the dppe reaction with **1** is tetranuclear $[Fe_2(CO)_5(\mu$-edt)$]_2(\kappa^1,\kappa^1$-dppe) (**6**) in which the diphosphine again occupies apical sites. Similar reactions of **1** and **2** with 1,1′-bis(diphenylphosphino)ferrocene (dppf) give single products namely, $Fe_2(CO)_5(\kappa^1$-dppf)(μ-edt) (**9**) and $Fe_2(CO)_5(\kappa^1$-dppf)(μ-tdt) (**10**), respectively, which are structurally similar to **3**. All seven complexes have been characterized by a combination of analytical and spectroscopic data together with single crystal X-ray diffraction analysis for **3**, **7**, **9** and **10**.

Keywords: Hydrogenase biomimetics, Diiron dithiolate complexes, dppm, dppe, dppf

Introduction

Over the past two decades there has been intense interest in the synthesis and structures of biomimetics of the active site (H-cluster) of the [FeFe]-hydrogenase enzyme (Fig. 1) [1-3] by far the majority of which contain a propanedithiolate (pdt) bridge [4-12]. The choice of the latter stems from the crystallographic work which shows that in the enzyme the two bridging sulfur atoms are linked by three other non-hydrogen atoms, and also the relative ease of preparation of pdt complexes as opposed to related adt ($SCH_2N(R)CH_2S$) species [2,3]. There are, however, some negative aspects to using pdt-bridged biomimetics. For example, in the solid-state the central methylene group is often disordered over two sites and this can result in relatively low quality X-ray crystallographic data [6,13]. In solution it is well-established that the central methylene unit is fluxional at room temperature "flipping" with a low activation barrier [13-15]. This can be problematic monitoring mechanistically important protonation reactions, since at the low temperatures required to observe intermediate hydride species, methylene fluxionality becomes slow on the NMR timescale leading to either a broadening of all resonances or, when sufficiently slow, a duplication of resonances resulting from the presence of isomers [6,14,15]. In our own work on $[Fe_2(CO)_3(\mu\text{-}\kappa^1,\kappa^2\text{-triphos})(\mu\text{-pdt})]$ (triphos = $(Ph_2PCH_2CH_2)_2PPh$) we have encountered this problem first hand [6]. Thus cooling to 183 K in CD_2Cl_2 in order to carry out a protonation experiment results in the freezing out of five isomers varying as a function of both phosphine and pdt orientations. The $^{31}P\{^1H\}$ NMR spectrum at this temperature is extremely complex (consisting of 15 resonances each of which shows at least one coupling) and consequently attempts to monitor the protonation at this temperature were fruitless. One possible partial solution to this problem is to exchange the pdt-bridge for the far more rigid ligand such as ethane- (edt), benzene- (bdt) or toluene (tdt) dithiolate thus simplifing the system and allowing important information to be more easily abstracted [16-19].

In comparison to the volume of work on pdt-bridged diiron hydrogenase biomimics, relatively little attention has been paid to related models containing an edt-bridge [18-21]. Recently, we have synthesized two edt-bridged diiron complexes $Fe_2(CO)_4(\kappa^2\text{-diamine})(\mu\text{-edt})$ containing diamine ligands, and investigated their electrocatalytic properties [21]. Experimental studies reveal that these edt-bridged complexes behave differently to their pdt-analogues, showing small but significant differences in their rates of protonation, leading to

different mechanisms for proton reduction [21]. This prompted us to extend our investigations on phosphine-substituted edt-bridged diiron complexes, and also to develop related toluene (tdt) dithiolate chemistry. Herein we report details of these together with structural studies in order to compare with the analogous pdt derivatives.

Experimental

Materials and Methods

All reactions were carried out under a nitrogen atmosphere using standard Schlenk techniques unless otherwise stated. Reagent grade solvents were dried by the standard procedures and were freshly distilled prior to use. $Fe_2(CO)_6$(μ-edt) (**1**) [22] and $Fe_2(CO)_6$(μ-tdt) (**2**) [22] were synthesized following published procedures. Infrared spectra were recorded on a Shimadzu FTIR 8101 spectrophotometer while the NMR spectra were recorded on a DPX 400 instrument. The chemical shifts were referenced to residual solvent resonances or external 85% H_3PO_4 in ^1H and ^{31}P spectra respectively. Elemental analyses were performed in the Microanalytical Laboratories of Wazed Miah Science Research Centre at Jahangirnagar University. Preparative thin layer chromatography was carried out on 1 mm plates prepared from silica gel GF254 (type 60, E. Merck) at Jahangirnagar University.

Reaction of 1 with dppm

$Fe_2(CO)_6$(μ-edt) (**1**) (100 mg, 0.268 mmol), Me_3NO (21 mg, 0.280 mmol) and dppm (104 mg, 0.271 mmol) was heated in boiling acetonitrile (15 mL) for 30 min. After cooling to room temperature, the volatiles were removed under reduced pressure and the residue chromatographed by TLC on silica gel. Elution with hexane/CH_2Cl_2 (7:3, v/v) developed two bands. The faster moving band afforded $Fe_2(CO)_5(\kappa^1$-dppm)(μ-edt) (**3**) (135 mg, 69%) as red crystals while the slower moving band gave $Fe_2(CO)_4$(μ-dppm)(μ-edt) (**4**) [9] (17 mg, 9%) as red crystals after recrystallization from hexane/CH_2Cl_2 at 4 °C.

$Fe_2(CO)_5(\kappa^1$-dppm)(μ-edt) (**3**): Anal. (%): Calcd. for $C_{32}H_{26}Fe_2O_5P_2S_2$: C, 52.77; H, 3.60%. Found: C, 53.29; H, 3.71%. IR (ν_{CO}, CH_2Cl_2): 2046 s, 1984 s, 1959 sh, 1931 w cm^{-1}. ^1H NMR ($CDCl_3$): δ 7.53 (m, 4H), 7.31-7.18 (m, 16H), 3.25 (dd, J 1.7, 8.0, 2H), 1.89 (m, 2H), 1.39 (m, 2H). $^{31}P\{^1H\}$ NMR ($CDCl_3$): δ 56.7 (d, J 86, 1P), –24.3 (d, J 86, 1P).

$Fe_2(CO)_4$(μ-dppm)(μ-edt) (**4**) [9]: Anal. (%): Calcd. for $C_{31}H_{26}Fe_2O_4P_2S_2$: C, 53.17; H, 3.74%. Found: C, 54.49; H, 3.79%. IR (ν_{CO}, CH_2Cl_2): 1991 m, 1959 s, 1924 m, 1906 w cm^{-1}. ^1H NMR ($CDCl_3$): δ 7.49 (m, 8H), 7.29 (m, 12H), 3.88 (m, 1H), 3.34 (m, 1H), 2.40 (br. s, 2H), 2.34 (br. s, 2H). $^{31}P\{^1H\}$ NMR ($CDCl_3$): δ 57.8 (s).

Reaction of 2 with dppm

An acetonitrile solution (15 mL) of $Fe_2(CO)_6$(μ-tdt) (**2**) (100 mg, 0.230 mmol), Me_3NO (17 mg, 0.230 mmol) and dppm (89 mg, 0.232 mmol) was heated to reflux for 30 min. The volatiles were removed by rotary evaporation and the residue chromatographed by TLC on silica gel. Elution with hexane/CH_2Cl_2 (7:3, v/v) developed only one band which yielded $Fe_2(CO)_4$(μ-dppm)(μ-tdt) (**5**) (95 mg, 54%) as red crystals after recrystallization from hexane/CH_2Cl_2 at 4 ^oC.

$Fe_2(CO)_4$(μ-dppm)(μ-tdt) (**5**): Anal. (%): Caled. for $C_{36}H_{28}Fe_2O_4S_2P_2$: C, 56.71; H, 3.70%. Found: C, 57.25; H, 3.76%. IR (ν_{CO}, CH_2Cl_2): 1994 s, 1964 s, 1930 s, 1911 w cm^{-1}. ^1H NMR ($CDCl_3$): δ 7.30 (m, 20H), 6.32 (d, J 8.4, 1H), 6.94 (d, J 8.4, 1H), 7.51 (s, 1H), 3.72 (m, 1H), 3.49 (m, 1H), 2.05 (s, 3H). $^{31}P\{^1H\}$ NMR ($CDCl_3$): δ 56.9 (s).

Reaction of 1 with dppe

A toluene solution (15 mL) of $Fe_2(CO)_6$(μ-edt) (**1**) (100 mg, 0.268 mmol), Me_3NO (42 mg, 0.559 mmol) and dppe (161 mg, 0.404 mmol) was heated to reflux for 30 min. The volatiles were removed under reduced pressure and the residue chromatographed by TLC on silica gel. Elution with hexane/CH_2Cl_2 (7:3, v/v) developed two bands. The faster moving band afforded $[Fe_2(CO)_5$(μ-edt)$]_2(\kappa^1,\kappa^1$-dppe) (**6**) [20] (27 mg, 19%) as red crystals while slower-moving band yielded $Fe_2(CO)_4(\kappa^2$-dppe)(μ-edt) (**7**) (48 mg, 25%) as green crystals after recrystallization from hexane/CH_2Cl_2 at 4 °C.

$[Fe_2(CO)_5$(μ-edt)$]_2(\kappa^1,\kappa^1$-dppe) (**6**) [20]: Anal. (%): Calcd. for $C_{40}H_{32}Fe_4O_{10}P_2S_4$: C, 44.23; H, 2.97%. Found: C, 44.64; H, 3.03%. IR (ν_{CO}, CH_2Cl_2): 2047 s, 1984 s, 1929 w cm^{-1}. ^1H NMR ($CDCl_3$): δ 7.47-7.32 (m, 20H), 2.40 (m, 4H), 1.85 (m, 4H), 1.30 (m, 4H). $^{31}P\{^1H\}$ NMR ($CDCl_3$): δ 58.4 (s).

$Fe_2(CO)_4(\kappa^2$-dppe)(μ-edt) (**7**): Anal. (%): Calcd. for $C_{32}H_{28}Fe_2O_4P_2S_2$: C, 53.80; H, 3.95%. Found: C, 54.32; H, 4.03%. IR (ν_{CO}, CH_2Cl_2): 2021 s, 1950 s, 1906 w cm^{-1}. ^1H NMR ($CDCl_3$): δ 7.89 (m, 4H), 7.48 (m, 6H), 7.28-7.20 (m, 10H), 2.82 (m, 2H), 2.62 (m, 2H), 1.74

(m, 2H), 1.21 (m, 2H). $^{31}P\{^{1}H\}$ NMR ($CDCl_3$): major isomer: δ 92.9 (s). minor isomer: δ 76.3 (s). major/minor = 11:1.

Reaction of 2 with dppe

An acetonitrile solution (15 mL) of $Fe_2(CO)_6$(μ-tdt) (**2**) (100 mg, 0.230 mmol), Me_3NO (17 mg, 0.230 mmol) and dppe (92 mg, 0.231 mmol) was heated to reflux for 10 min. The volatiles were removed by rotary evaporation and the residue chromatographed by TLC on silica gel. Elution with hexane/CH_2Cl_2 (4:1, v/v) developed only one band which yields $Fe_2(CO)_4(\kappa^2$-dppe)(μ-tdt) (**8**) (25 mg, 14 %) as red crystals after recrystallization from hexane/CH_2Cl_2 at 4 ^{o}C.

$Fe_2(CO)_4(\kappa^2$-dppe)(μ-tdt) (**8**): Anal. (%): Caled. for $C_{37}H_{30}Fe_2O_4S_2P_2$: C, 57.24; H, 3.90%. Found: C, 57.97; H, 3.98%. IR (ν_{CO}, CH_2Cl_2): 2021 s, 1950 m, 1906 m cm^{-1}. ^{1}H NMR ($CDCl_3$): δ 8.03 (d, J 8.4, 1H), 7.97 (s, 1H), 7.81 (m, 4H), 7.49 (m, 6H), 7.28 (m, 2H), 7.14 (m, 8H), 6.96 (d, J 8.4, 1H), 2.82 (m, 2H), 2.62 (m, 2H), 2.37 (s, 3H). $^{31}P\{^{1}H\}$ NMR ($CDCl_3$): major isomer: δ 89.3 (s); minor isomer: δ 34.3 (s). major/minor = 8:1.

Reaction of 1 with dppf

To an acetonitrile solution (15 mL) of $Fe_2(CO)_6$(μ-edt) (**1**) (100 mg, 0.268 mmol) and dppf (149 mg, 0.269 mmol) was added Me_3NO (21 mg, 0.280 mmol) and the mixture was heated to reflux for 1 h. After cooling to room temperature, the solvent was removed by rotary evaporation and the residue chromatographed by TLC on silica gel. Elution with hexane/CH_2Cl_2 (1:1, v/v) developed one band which yields $Fe_2(CO)_5(\kappa^1$-dppf)(μ-edt) (**9**) (145 mg, 60%) as red crystals after recrystallization from hexane/CH_2Cl_2 at 4 °C.

$Fe_2(CO)_5(\kappa^1$-dppf)(μ-edt) (**9**): Anal. (%): Calcd. for $C_{41}H_{32}Fe_3O_5P_2S_2$: C, 54.82; H, 3.59%. Found: C, 55.39; H, 3.66%. IR (ν_{CO}, CH_2Cl_2): 2046 s, 1984 s, 1931 w cm^{-1}. ^{1}H NMR ($CDCl_3$): δ 7.55-7.14 (m, 20H), 6.45 (d, J 6.4, 1H), 6.14 (s, 1H), 6.03 (d, J 6.4, 1H), 4.52 (br. s, 1H), 4.39 (br. s, 1H), 4.35 (br. s, 1H), 4.29 (br. s, 1H), 4.21 (br. s, 1H), 4.15 (br. s, 1H), 3.94 (br. s, 1H), 3.77 (br. s, 1H), 1.83 (s, 3H). $^{31}P\{^{1}H\}$ NMR ($CDCl_3$): δ 53.5 (s, 1P), –16.3 (s, 1P).

Reaction of 2 with dppf

An acetonitrile solution (15 mL) of $Fe_2(CO)_6(\mu$-tdt) (100 mg, 0.230 mmol), Me_3NO (17 mg, 0.230 mmol) and dppf (128 mg, 0.231 mmol) was heated to reflux for 1 h. The volatiles were removed by rotary evaporation and the residue chromatographed by TLC on silica gel. Elution with hexane/CH_2Cl_2 (9:1, v/v) developed only one band which yielded $Fe_2(CO)_5(\kappa^1$-dppf)(μ-tdt) (**10**) (120 mg, 54%) as red crystals after recrystallization from hexane/CH_2Cl_2 at 4 ^oC.

$Fe_2(CO)_5(\kappa^1$-dppf)(μ-tdt) (**10**): Anal. (%): Caled. for $C_{46}H_{34}Fe_3O_5P_2S_2$: C, 57.53; H, 3.57%. Found: C, 58.05; H, 3.62%. IR (ν_{CO}, CH_2Cl_2): 2049 s, 1989 s, 1932 m cm^{-1}. ^1H NMR ($CDCl_3$): δ 7.56-7.15 (m, 20H), 6.58 (d, J 8.4, 1H), 6.15 (s, 1H), 5.94 (d, J 8.4, 1H), 4.45 (br. s, 1H), 4.39 (br. s, 1H), 4.35 (br. s, 1H), 4.29 (br. s, 1H), 4.21 (br. s, 1H), 4.15 (br. s, 1H), 3.94 (br. s, 1H), 3.77 (br. s, 1H), 1.84 (3H, s). $^{31}P\{^1H\}$ NMR ($CDCl_3$): δ 53.5 (s, 1P), –16.3 (s, 1P).

X-ray crystallography

Single crystals of **3**, **7**, **9** and **10** suitable for X-ray diffraction were grown by slow diffusion of hexane into a dichloromethane solution at 4 °C. All geometric and crystallographic data were collected at 150(2) K on a Bruker SMART APEX CCD diffractometer using Mo-Kα radiation (λ = 0.71073 Å) [23]. Data reduction and integration were carried out with SAINT+ [24] and absorption corrections were applied using the program SADABS [25]. Numerical (based on the real shape of the crystals) absorption correction was applied in all cases followed by the multi-scan SADABS procedure [25]. The structures were solved by direct methods and refined by full-matrix least squares on F^2 [26,27]. All non-hydrogen atoms were refined anisotropically for **3**, **7** and **10**. The hydrogen atoms were placed in the calculated positions and their thermal parameters were linked to those of the atoms to which they were attached (riding model). The crystal of **9** decomposed considerably during the experiment leading to poor data collection, so the atoms of **9** were modeled isotropically with a common thermal parameter and no hydrogen atoms were included in this part of the model. The SHELXTL PLUS V6.10 program package was used for structure solution and refinement [27]. Final difference maps did not show any residual electron density of stereochemical significance. The details of the data collection and structure refinement are given in Table 1.

Results and discussion

Reaction 1 and 2 with dppm

Me_3NO initiated reaction between $Fe_2(CO)_6$(μ-edt) (**1**) and dppm in acetonitrile resulted in the isolation of $Fe_2(CO)_5(\kappa^1$-dppm)(μ-edt) (**3**) and $Fe_2(CO)_4$(μ-dppm)(μ-edt) (**4**) in 69 and 9% yields, respectively, after chromatographic separation and work up (Scheme 1). In contrast a similar reaction between $Fe_2(CO)_6$(μ-tdt) (**2**) and dppm yielded only $Fe_2(CO)_4$(μ-dppm)(μ-tdt) (**5**) in 54% yield (Scheme 2), indicating that the removal of the second carbonyl from the molecule by phosphine is relatively faster in tdt-complex **2** as compared to that in edt-complex **1**. Complex **4** has been previously reported and structurally characterized by Kabir and Hogarth, isolated from the reaction between **1** and dppm in boiling toluene as the only product [9]. Here we have characterized **3** and **5** by a combination of analytical and spectroscopic data together with single crystal X-ray diffraction studies for **3**.

The solid-state molecular structure of **3** is depicted in Fig. 2 with the caption containing selected bond distances and angles. The molecule contains a diiron framework bridged by an edt ligand in addition to five terminal carbonyls and a dangling dppm ligand which complete the coordination sphere of the molecule. The Fe─Fe bond distance of 2.5052(6) Å in **3** is the same as that of the parent hexacarbonyl **1** [2.5032 (5) Å] [28] (within experimental error). The Fe─S bond distances of **3** are also very similar to those observed in **1** [28]. The dppm ligand is apically bonded to a single iron atom using one phosphorus atom thus acting as a monodentate ligand, and the Fe─P bond distance of 2.2258(8) Å in **3** is within the range reported for related diiron-dithiolate complexes [5-15]. Almost a decade ago, Sun and co-workers reported the crystal structure of the pdt and adt analogues of **3** namely $Fe_2(CO)_5(\kappa^1$-dppm)(μ-pdt) and $Fe_2(CO)_5(\kappa^1$-dppm)(μ-$SCH_2N(R)CH_2S$) (R = $CH_2CH_2CH_3$) [29]. Whilst in the adt analogue the dppm is bound to an apical site akin to that observed in **3**, the diphosphine is found to be bonded to a single iron through a basal coordination site in the pdt complex [29]. The solution spectroscopic data of **3** also indicate that the solid-state structure persists in solution. The carbonyl region of the IR spectrum shows characteristic absorptions pattern of $Fe_2(CO)_5$(phosphine)(μ-dithiolate) complexes, while the $^{31}P\{^1H\}$ NMR spectrum displays two well separated doublets at 56.7 and –24.3 ppm (J 86 Hz) for the coordinated and non-coordinated ^{31}P nuclei respectively. The ^1H NMR spectrum is not very informative but it

shows separate resonances for the methylene moieties of dppm and edt ligands in addition to phenyls proton resonances in the aromatic region.

Complex **5** can be readily characterized by its IR spectra which show four absorption bands: three sharp and strong absorptions at 1994, 1964 and 1930 cm^{-1}, and a weak absorption 1911 cm^{-1}. It shows a single resonance in the $^{31}P\{^{1}H\}$ NMR spectrum at 56.9 ppm since both the phosphorus atoms of the dppm ligand have an identical environment in this molecule. In addition to resonances in the aromatic region for the phenyl protons of dppm ligand, the ^{1}H NMR spectrum of **5** also shows a multiplet at 3.49 ppm (integrated to two protons) and a singlet at 2.05 ppm (integrated to three protons) which are attributed to the methylene and methyl protons of the dppm and tdt ligands, respectively.

Reactions of 1 and 2 with dppe

Similar reactions described as above between **1** and dppe yielded the tetrairon $[Fe_2(CO)_5(\mu\text{-edt})]_2(\kappa^1,\kappa^1\text{-dppe})$ (**6**) [20] and diiron $Fe_2(CO)_4(\kappa^2\text{-dppe})(\mu\text{-edt})$ (**7**) in 19 and 25% yields respectively, whereas reaction between **2** and dppe afforded only the chelate analogue $Fe_2(CO)_4(\kappa^2\text{-dppe})(\mu\text{-tdt})$ (**8**) in 14% yield. We could not isolate any complex similar to **3** from the reaction between **1** and dppe in which the dppe ligand is coordinated in monodentate fashion. The increased flexibility due to the presence of an extra methylene group in the backbone helps dppe to coordinate with a second diiorn unit which is not possible for dppm. The tetrairon complex **6** has been previously reported and structurally characterized [20]. Here, we have characterized **7** and **8** by a combination of analytical and spectroscopic data together with X-ray diffraction analysis for **7**. Both **7** and **8** show three absorption bands in the carbonyl region of their IR spectra which is characteristic of $Fe_2(CO)_4(\kappa^2\text{-diphophine})(\mu\text{-dithiolate})$ complexes. The ^{1}H NMR spectra of both complexes are uninformative which show resonances attributed to the methylene protons of the dppe ligand in addition to other proton resonances. Their $^{31}P\{^{1}H\}$ NMR spectra indicate that both exist in two isomeric forms in solution due to trigonal twist of the $Fe(CO)(\kappa^2\text{-dppe})$ unit commonly observed in this type of complexes (Chart) [9,10,15]. Both display a large singlet (92.9 ppm for **7** and 89.3 ppm for **8**) together with a smaller singlet (76.3 ppm for **7** and 34.3 ppm for **8**) in their $^{31}P\{^{1}H\}$ NMR spectra which are ascribed to the basal-apical and dibasal isomers of **7** and **8**, being formed in an approximate 11:1 and 8:1 ratio, respectively. Such isomerism has been previously observed in complexes of this type with exchange between isomers being slow on the NMR

time scale [9,10,15]. The major isomer in solution for diphosphines with flexible backbone such as dppe utilized in this study which are able to span apical and basal sites is the basal-apical isomer [10,15]. Complex **7** is also found to adopt basal-apical configuration in the solid-state (see later) which is in accord with this observation.

The solid-state molecular structure of **7** is shown in Fig. 3 with the caption containing selected bond distances and angles. The molecule consists of a diiron core ligated by four carbonyls, a dppe and a bridging edt ligand. The molecule structure of **7** is very similar to that of its pdt analogue, $Fe_2(CO)_4(\kappa^2$-dppe)(μ-pdt) [30]. The diphosphine chelates one iron occupying the apical and one of the basal coordination sites in the solid-state with a bite angle of 86.91(2)° which is quite similar to 87.7(4)° observed in $Fe_2(CO)_4(\kappa^2$-dppe)(μ-pdt) [30]. The Fe─Fe and Fe─P bond distances in **7** [Fe(1)─Fe(2) 2.5502(5) Å, Fe(1)─P(1) 2.1822(6) Å and Fe(1)─P(2) 2.2089(6) Å] are also quite similar to those reported for its pdt analogue $Fe_2(CO)_4(\kappa^2$-dppe)(μ-pdt) [30] [Fe(1)─Fe(2) 2.547(7) Å, Fe(1)─P(1) 2.190(1) Å and Fe(1)─P(2) 2.231(1) Å].

Reactions of diiron complexes 1 and 2 with dppf

Recently, redox-active ligands containing ferrocene moiety have been successfully used in the diiron biomimics as a surrogate of ferrodoxin clusters by several groups [11,31,32], which prompted researchers to synthesis and study more biomimetic models containing redox-active ligands based on ferrocene [17,33,34]. Couple of years ago, we examined the reaction of $Fe_2(CO)_6$(μ-pdt) with dppf in boiling toluene and observed that the tetrairon complex $[Fe_2(CO)_5$(μ-pdt)$]_2(\kappa^1,\kappa^1$-dppf) formed very quickly which converted into the diiron complex $Fe_2(CO)_4$(μ-dppf)(μ-pdt) upon prolonged heating at the same temperature [11]. Very recently, Kaur- Ghumaan et al. studied the reactivity of the tdt complex **2** with dppf and reported that room temperature reaction between **2** and dppf (in 2:1 molar ratio) in presence of one equivalent $Me_3NO{\cdot}2H_2O$ yielded three products: the tetrairon complex $[Fe_2(CO)_5$(μ-tdt)$]_2(\kappa^1,\kappa^1$-dppf) and the diron complexes $Fe_2(CO)_5(\kappa^1$-dppf)(μ-tdt) (**10**) and $Fe_2(CO)_5(\kappa^1$-dppfO)(μ-tdt) [17]. The later formed due to the oxidation of dppf by $Me_3NO{\cdot}2H_2O$ [17]. Here, we have investigated the reactivity of both **1** and **2** towards dppf using slightly different reaction conditions and obtained a single product in each case. Thus, the equimolar reaction between **1** or **2** and dppf in presence of one equivalent of Me_3NO in boiling acetonitrile only led to the formation of $Fe_2(CO)_5(\kappa^1$-dppf)(μ-edt) (**9**) (60%) or $Fe_2(CO)_5(\kappa^1$-dppf)(μ-tdt) (**10**)

[17] (54%), respectively, after chromatographic separation and work up (Schemes 1 and 2). Complex **10** has been previously characterized by analytical and spectroscopic data by Kaur-Ghumaan et al. [17]. Here we have carried out single crystal X-ray diffraction analysis of both dppf-substituted complexes **9** and **10**, the results of which are shown in Figs. 4 and 5. Although the refinement of the structure of **9** is poor since the crystal decomposed considerably during data collection, the structure gives sufficient information about the geometry of the molecule and the orientation of the ligands on the diiron framework.

Both molecules contain a diiron core ligated by five carbonyls, a dithiolate ligand and a dppf ligand. The Fe─Fe bond distance of 2.5164(13) Å in **9** is slightly longer than that in **10** [2.4877(6) Å] since the later is bridged by comparatively more rigid tdt ligand. The dppf ligand is bonded to an iron through the apical coordination site in κ^1-fashion thus acting as a monodentate phosphine in both molecules. The Fe─P bond distance of both molecules are identical within the experimental error [2.2348(19) Å in **9** and 2.2374(8) Å], and are similar to those observed in related dppf-substituted diiron dithiolate complexes such as $Fe_2(CO)_5(\kappa^1$-dppfO)(μ-tdt) [2.2419(6) Å] [17] and $Fe_2(CO)_4$(μ-dppf)(μ-pdt) [2.2468(6) Å] [11]. In both, the geometry around each iron can be best described as distorted square pyramidal which a is common feature observed in diiron dithiolate complexes, and the Fe─S bond distances observed in **9** and **10** are quite similar to those found in related complexes. The solution spectroscopic data of both complexes are in accord with the solid- state structure. The IR spectra of both show three absorption bands in the carbonyl region characteristic for $Fe_2(CO)_5$(phosphine)(μ-dithiolate) complexes, whilst their $^{31}P\{^1H\}$ NMR spectra displays two well-separated singlets for the coordinated and non-coordinated phosphorus of dppf ligand.

Conclusions

The reactivity of two diiron dithiolate complexes, $Fe_2(CO)_6$(μ-edt) (**1**) and $Fe_2(CO)_6$(μ-tdt) (**2**), toward three diphosphines (dppm, dppe and dppf) have been investigated which resulted in the isolation of a number of products. This reveals that the nature of the products is highly sensitive to the diphosphine used in the study. As we know, the dppm ligand in which the donor phosphorus atoms are separated by single CH_2 unit prefers bridging coordination mode thus led to the formation of product where the two iron atoms are bridged by the diphosphine.

In contrast, the dppe in which there are two CH_2 units between phosphorus atoms formed products where the diphosphine chelates a single iron. The dppf ligand shows only monodentate coordination mode in the present study since prolonged heating at high temperature is usually required to bind both donor atoms of dppf with the diiron core [11].

Supplementary Data

Crystallographic data for the structural analyses have been deposited with the Cambridge Crystallographic Data centre. CCDC 1497271, CCDC 1497272, CCDC 1497361 and CCDC 1497358 contain supplementary crystallographic data for compound **3**, **7**, **9** and **10** respectively. These data can be obtained free of charge from the Director, CCDC, 12 Union Road, Cambridge, CB2 1 EZ, UK (fax: +44-1223-336033; Email: deposit@ccdc.cam.ac.uk or www: http://www.ccdc.ac.uk).

Acknowledgments

This research has been partly sponsored by the Ministry of Education, Government of the People's Republic of Bangladesh.

References

1 (a) Adams MWW, Stiefel EI (1998) Science 282:1842; (b) Cammack R (1999) Nature 397:214; (c) Frey M (2002) ChemBioChem 3:153

2 (a) Peters JW, Lanzilotta WN, Lemon BJ, Seefeldt LC (1998) Science 282:1853; (b) Nicolet Y, Piras C, Legrand P, Hatchikian CE, Fontecillacamps JC (1999) Structure 7:13

3 (a) Volbeda A, Charon MH, Piras C, Hatchikian CE, Frey M, Fontecillacamps JC (1995) Nature 373:580; (b) Shima S, Pilak O, Vogt S, Schick M, Stagni MS, Meyer-Klaucke W, Warkentin E, Thauer RK, Ermler U (2008) Science 321:572; (c) Shima S, Lyon EJ, Thauer RK, Mienert B, Bill E (2005) J Am Chem Soc 127:10430

4 For some reviews of this area see: (a) Tard C, Pickett CJ (2009) Chem Rev 109:2245; (b) Georgakaki IP, Thomson L M, Lyon EJ, Hall MB, Darensbourg MY (2003) Coord Chem Rev 238-239 255; (c) Evans DJ, Pickett CJ (2003) Chem Soc Rev 32:268; (d) Rauchfuss TB (2004) Inorg Chem 43:14; (e) Sun L, Åkermark B, Ott S (2005) Coord Chem Rev 249:1653; (f) Liu X, Ibrahim SK, Tard C, Pickett CJ (2005) Coord Chem Rev 249:1641; (g) Capon J-F,

Gloaguen F, Schollhammer P, Talarmin J (2005) Coord Chem Rev 249:1664; (h) Felton GAN, Mebi CA, Petro BJ, Vannucci AK, Evans DH, Glass RS, Lichtenberger DL (2009) J Organomet Chem 694:2681; (i) Heinekey DM (2009) J Organomet Chem 694:2671; (j) Holladay JD, Hu J, King DL, Wang Y (2009) Catal Today 139:244

5 Adam FI, Hogarth G, Richards I, Sanchez B E (2007) Dalton Trans 2495

6 Adam FI, Hogarth G, Richards I (2007) J Organomet Chem 692:3957

7 Hogarth G, Richards I (2007) Inorg Chem Commun 10:66

8 Adam FI, Hogarth G, Kabir SE, Richards I (2008) C R Chim 11:890

9 Hogarth G, Kabir SE, Richards I (2010) Organometallics 29:6559

10 Ghosh S, Hogarth G, Hollingsworth N, Holt KB, Richards I, Richmond MG, Sanchez BE, Unwin DG (2013) Dalton Trans 42:6775

11 Ghosh S, Hogarth G, Hollingsworth N, Holt KB, Kabir S E, Sanchez BE (2014) Chem Commun 50:945

12 Ghosh S, Sanchez BE, Richards I, Haque MN, Holt KB, Richmond MG, Hogarth G (2016) J Organomet Chem 812:247

13 Si Y, Charreteur K, Capon J-F, Gloaguen F, Pétillon FY, Schollhammer P, Talarmin J (2010) J Inorg Biochem, 104:1038

14 Ezzaher S, Capon J-F, Gloaguen F, Kervarec N, Pétillon F Y, Pichon R, Schollhammer P, Talarmin J (2008) C R Chimie 11:906

15 Capon J-F, Gloaguen F, Pétillon FY, Schollhammer P, Talarmin J (2008) Eur J Inorg Chem 4671

16 Capon J-F, Gloaguen F, Schollhammer P, Talarmin J (2004) J Electroanal Chem 566:241

17 Kaur-Ghumaan S, Sreenithya A, Sunoj RB (2015) J Chem Sci 127:557

18 Ghosh S, Unwin DG, Basak-Modi S, Holt KB, Kabir SE, Nordlander E, Richmond MG, Hogarth G (2014) Organometallics 33:1356

19 Ghosh S, Hogarth G, Holt KB, Kabir SE, Rahaman A, Unwin DG (2011) Chem Commun 47:11222

20 Liu X-F, Jiang Z-Q, Jia Z-J (2012) Polyhedron 33:166

21 Ghosh S, Rahaman A, Holt KB, Nordlander E, Richmond MG, Kabir SE, Hogarth G (2016) Polyhedron in press (http://dx.doi.org/10.1016/j.poly.2016.05.015)

22 Winter A, Zsolnai L, Huttner G (1982) Z Naturforsch 37b:1430

23 APEX2 Version 2.0-2, Bruker AXS Inc.: Madison, WI, 2005

24 SAINT Version 7.23A; Bruker AXS Inc.: Madison, WI, 2005

25 Sheldrick G M, SADABS Version 2004/1, University of Göttingen, 2004

26 Program XS from SHELXTL package, V. 6.12, Bruker AXS Inc.: Madison, WI, 2001

27 Program XL from SHELXTL package, V. 6.12, Bruker AXS Inc.: Madison, WI, 2001

28 Kabir SE, Rahman AFMM, Parvin J, Malik KMA (2003) Indian J Chem 42A: 2518

29 Gao W, Ekstrŏm J, Liu J, Chen C, Eriksson L,Weng L, Åkermark B, Sun L (2007) Inorg Chem, 46:1981

30 Ezzaher S, Capon J-F, Gloaguen F, Pétillon FY, Schollhammer P, Talarmin J, Pichon R, Kervarec N (2007) Inorg Chem 46:3426

31 Camara JM, Rauchfuss TB (2012) Nat Chem, 4:26.

32 Camara JM, Rauchfuss TB, J Am Chem Soc, 133 (2011) 8098

33 Gimbert-Suriñach C, Bhadbhade M, Colbran SB (2012) Organometallics 31:3480

34 Liu Y-C, Lee C-H, Lee G-H, Chiang M-H (2011) Eur J Inorg Chem 1155

Table 1 Crystal data and structure refinement details for compounds (**3**), (**7**), (**9**) and (**10**)

Complex	**3**·CH_2Cl_2	**7**	**9**	**10**
Empirical formula	$C_{33}H_{28}Cl_2Fe_2O_5P_2S_2$	$C_{32}H_{28}Fe_2O_4P_2S_2$	$C_{41}H_{32}Fe_3O_5P_2S_2$	$C_{46}H_{34}Fe_3O_5P_2S_2$
Formula weight	813.21	714.30	898.28	960.34
Temperature (K)	150(2)	150(2)	150(2)	150(2)
Wavelength (Å)	0.71073	0.71073	0.71073	0.71073
Crystal system	triclinic	monoclinic	monoclinic	triclinic
Space group	*P*1bar	$P2_1/n$	$P2_1/c$	*P*1bar
Unit cell dimensions				
a (Å)	11.7308(10)	12.0601(12)	11.9306(15)	13.2014(17)
b (Å)	11.7655(10)	15.1211(16)	17.230(2)	13.7267(18)
c (Å)	12.5708(10)	17.2738(18)	18.615(2)	14.0341(18)
α (°)	86.9620(10)	90	90	112.962(2)
β (°)	81.9960(10)	98.281(2)	102.550(3)	107.333(2)
γ (°)	80.7460(10)	90	90	103.637(2)
Volume ($Å^3$)	1694.9(2)	3117.2(6)	3735.2(8)	2048.2(5)
Z	2	4	4	2
Density (calculated) (Mg/m^3)	1.593	1.522	1.597	1.557
Absorption coefficient (mm^{-1})	1.272	1.204	1.393	1.276
F(000)	828	1464	1832	980
Crystal size (mm^3)	0.14 × 0.12 × 0.03	0.18 × 0.16 × 0.08	0.04 × 0.03 × 0.01	0.22 × 0.10 × 0.08
Θ range for data collection (°)	2.44 to 28.29	2.95 to 28.31	2.20 to 28.28	2.67 to 28.23
Index ranges	$-15 \le h \le 15$, $-15 \le k \le 15$, $-16 \le l \le 16$	$-15 \le h \le 15$, $-19 \le k \le 20$, $-23 \le l \le 22$	$-15 \le h \le 15$, $-24 \le k \le 22$, $-24 \le l \le 24$	$-17 \le h \le 17$, $-17 \le k \le 17$, $-18 \le l \le 18$
Reflections collected	14494	26144	32465	16950
Independent reflections [R_{int}]	7729 [R_{int} = 0.0261]	7432 [R_{int} = 0.0377]	8952 [R_{int} = 0.1279]	9167 [R_{int} = 0.0301]
Max. and min. transmission	0.9628 and 0.8420	0.9099 and 0.8125	0.9862 and 0.9464	0.9048 and 0.7666
Data / restraints / parameters	7729 / 0 / 415	7432 / 0 / 379	8952 / 0 / 478	9167 / 0 / 523
Goodness of fit on F^2	1.115	1.000	1.127	1.029
Final *R* indices [$I > 2\sigma(I)$]	R_1 = 0.0419, wR_2 = 0.1294	R_1 = 0.0387, wR_2 = 0.0893	R_1 = 0.0956, wR_2 = 0.1589	R_1 = 0.0434, wR_2 = 0.0997
R indices (all data)	R_1 = 0.0514, wR_2 = 0.1450	R_1 = 0.0546, wR_2 = 0.0952	R_1 = 0.1468, wR_2 = 0.1776	R_1 = 0.0595, wR_2 = 0.1058
Largest diff. peak and hole (e. $Å^{-3}$)	0.880 and –0.767	0.597 and –0.408	0.921 and –0.683	0.634 and –0.330

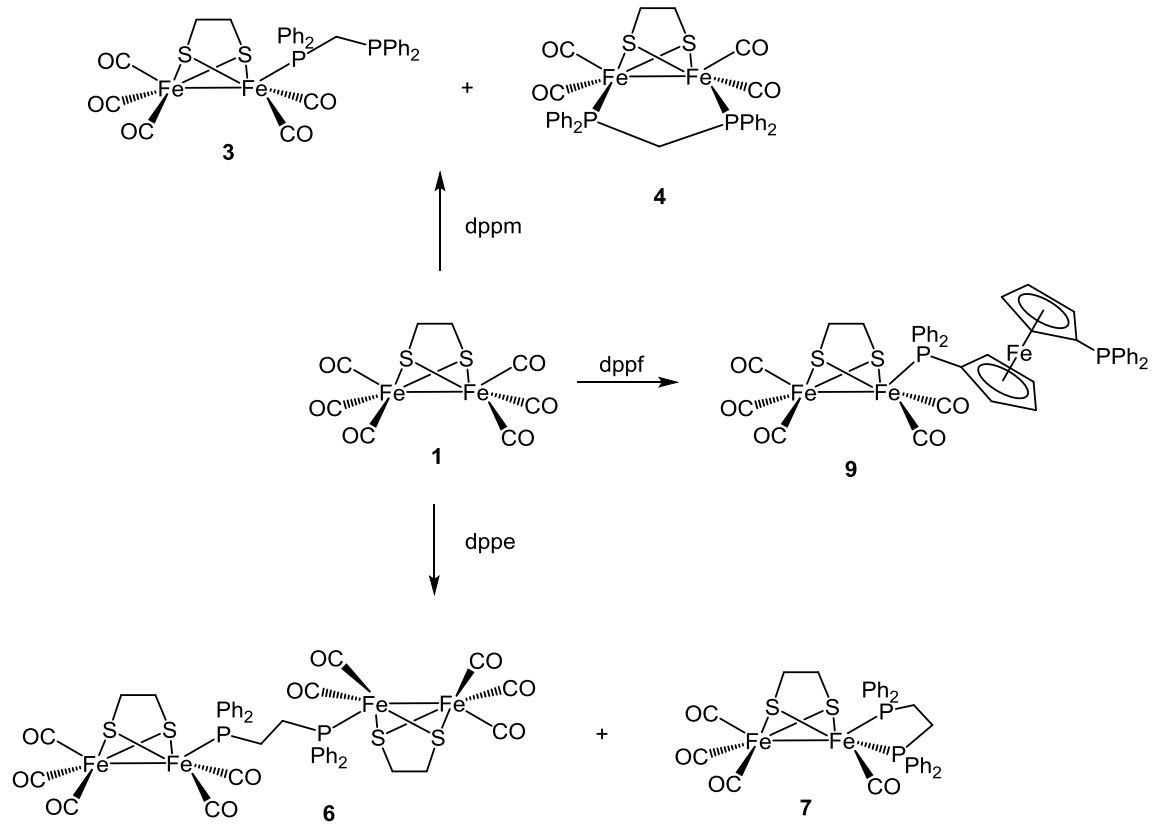

Scheme 1 Reactions of $Fe_2(CO)_6$(μ-edt) (**1**) with various diphosphines

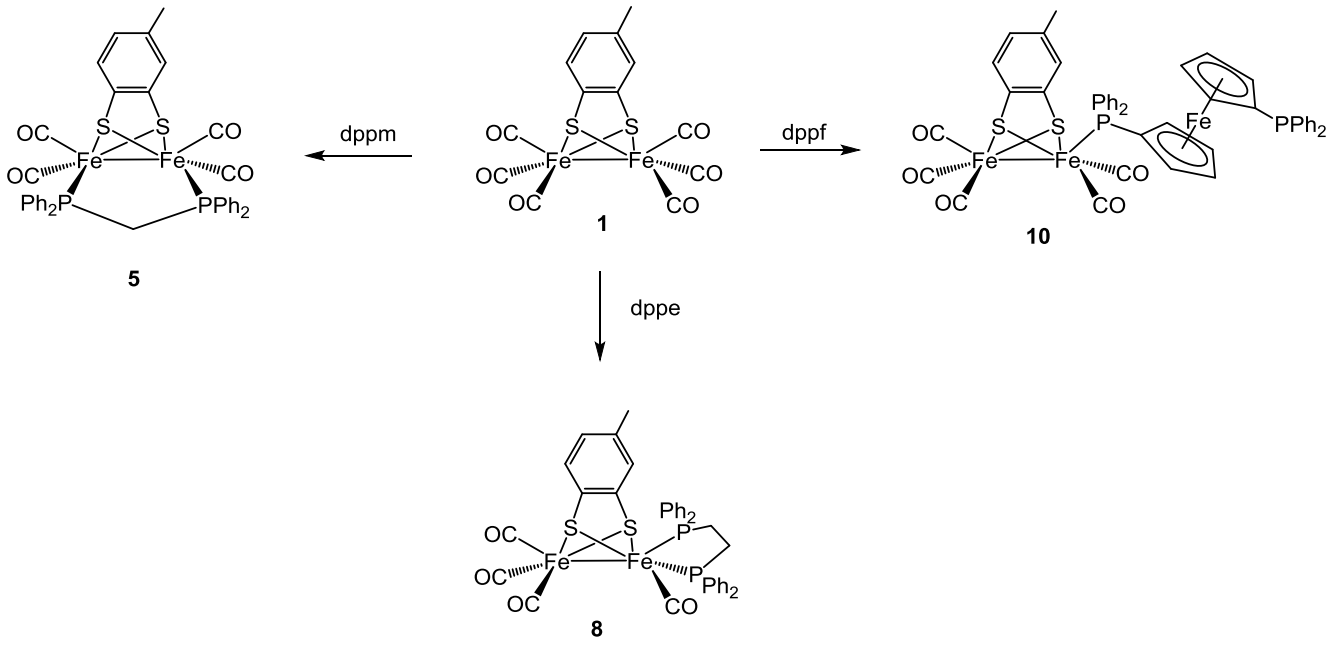

Scheme 2 Reactions of $Fe_2(CO)_6$(μ-edt) (**2**) with various diphosphines

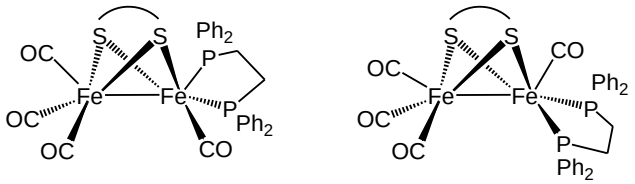

Chart Basal-apical and dibasal isomers of $Fe_2(CO)_4(\kappa^2$-diphosphine)(μ-dithiolate) complexes

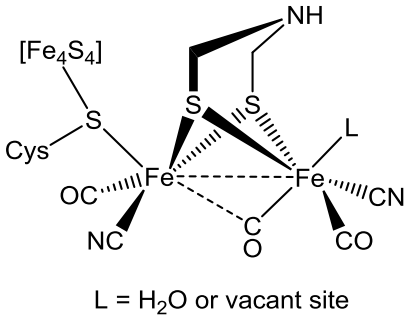

Fig. 1 Active site of [FeFe]-hydrogenase

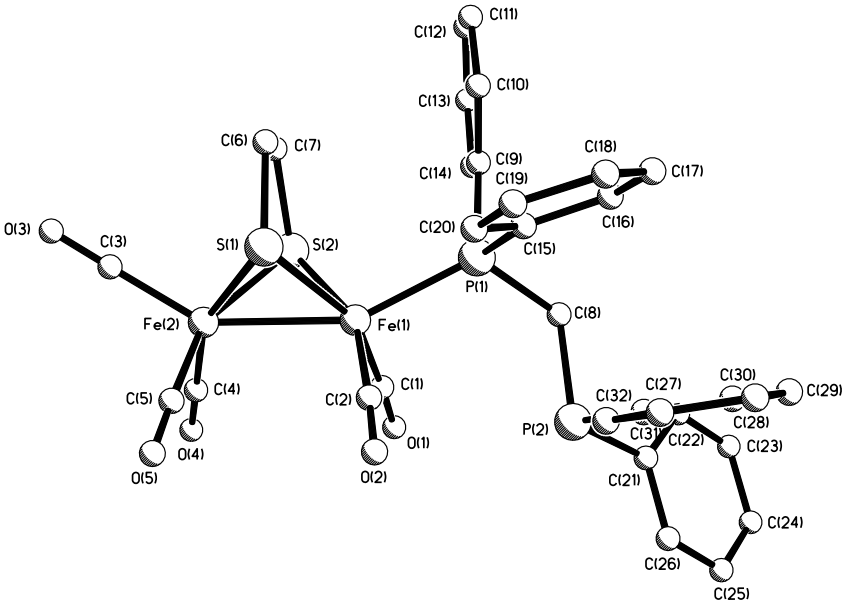

Fig. 2 The solid-state molecular structure of $Fe_2(CO)_5(\kappa^1$-dppm)(μ-edt) (**3**). Ring hydrogen atoms are omitted for clarity. [Selected bond distances (Å) and angles (°): Fe(1)─Fe(2)

2.5052(6), Fe(1)─P(1) 2.2258(8), Fe(1)─S(1) 2.2491(8), Fe(1)─S(2) 2.2481(8), Fe(2)─S(1) 2.2518(8), Fe(2)─S(2) 2.2525(8); P(1)─Fe(1)─Fe(2) 153.67(3), P(1)─Fe(1)─S(1) 106.31(3), P(1)─Fe(1)─S(2) 104.42(3), P(1)─Fe(1)─C(1) 97.40(10), P(1)─Fe(1)─C(2) 98.22(10)].

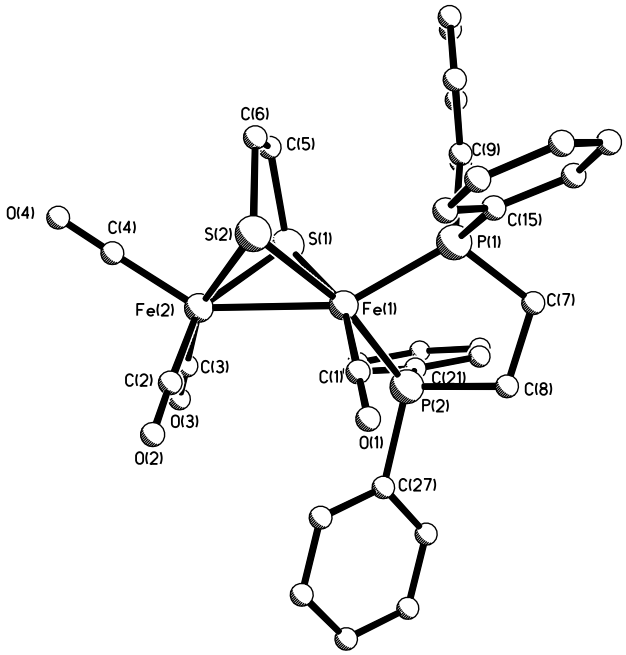

Fig. 3 The solid-state molecular structure of $Fe_2(CO)_4(\kappa^2$-dppe)(μ-edt) (**7**). Ring hydrogen atoms are omitted for clarity. [Selected bond distances (Å) and angles (°): Fe(1)─Fe(2) 2.5502(5), Fe(1)─P(1) 2.1822(6), Fe(1)─P(2) 2.2089(6), Fe(1)─S(1) 2.2445(6), Fe(1)─S(2) 2.2392(6), Fe(2)─S(1) 2.2530(6), Fe(2)─S(2) 2.2529(7); P(1)─Fe(1)─Fe(2) 151.34(2), P(1)─Fe(1)─S(1) 103.62(2), P(1)─Fe(1)─S(2) 105.11(2), P(1)─Fe(1)─P(2) 86.91(2), P(1)─Fe(1)─C(1) 96.33(8)].

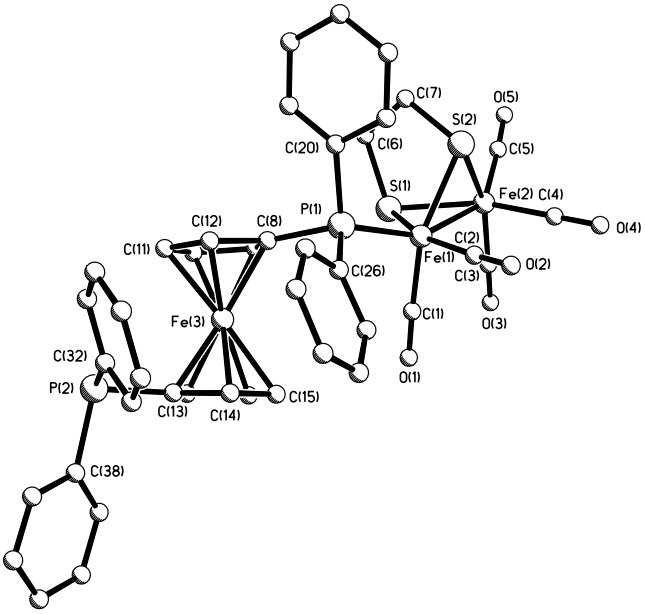

Fig. 4 The solid-state molecular structure of $Fe_2(CO)_5(\kappa^1$-dppf)(μ-edt) (**9**). Ring hydrogen atoms are omitted for clarity. [Selected bond distances (Å) and angles (°): Fe(1)─Fe(2) 2.5164(13), Fe(1)─P(1) 2.2348(19), Fe(1)─S(1) 2.2510(19), Fe(1)─S(2) 2.2540(19), Fe(2)─S(1) 2.2439(19), Fe(2)─S(2) 2.2463(19); P(1)─Fe(1)─Fe(2) 152.59(6), P(1)─Fe(1)─S(1) 105.32(7), P(1)─Fe(1)─S(2) 104.53(7), P(1)─Fe(1)─C(1) 100.5(2), P(1)─Fe(1)─C(2) 94.9(2)].

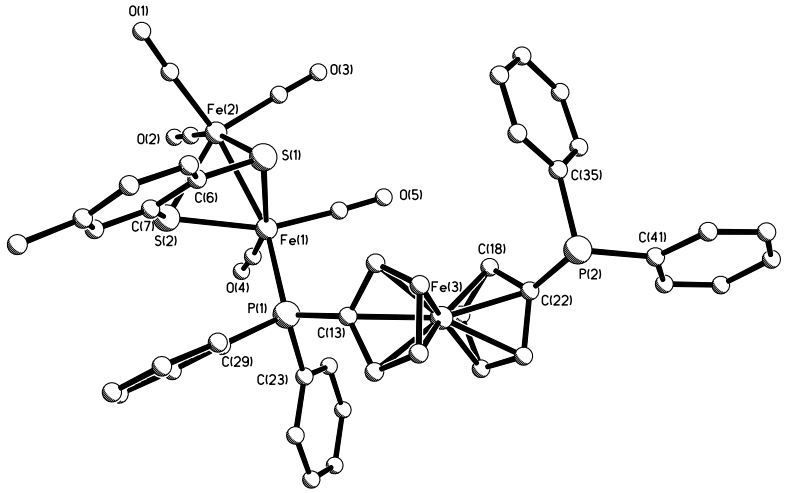

Fig. 5 The solid-state molecular structure of $Fe_2(CO)_5(\kappa^1$-dppf)(μ-tdt) (**10**). Ring hydrogen atoms are omitted for clarity. [Selected bond distances (Å) and angles (°): Fe(1)─Fe(2) 2.4877(6), Fe(1)─P(1) 2.2374(8), Fe(1)─S(1) 2.2854(9), Fe(1)─S(2) 2.2696(8), Fe(2)─S(1)

2.2812(9), Fe(2)─S(2) 2.2844(9); P(1)─Fe(1)─Fe(2) 152.96(3), P(1)─Fe(1)─S(1) 103.82(3), P(1)─Fe(1)─S(2) 103.99(3), P(1)─Fe(1)─C(4) 98.98(10), P(1)─Fe(1)─C(5) 97.49(9)].

Graphical abstract

Reactivity $Fe_2(CO)_6$(μ-edt) and $Fe_2(CO)_6$(μ-tdt) toward a series of diphosphines have been investigated from which a number of different kind of products are isolated and characterized.